European Review for Medical and Pharmacological Sciences 2022; 26: 3840-3848

MR imaging properties of breast cancer molecular subtypes

A. SEYFETTIN[1], İ. DEDE[2], S. HAKVERDI[3], B. DÜZEL ASIG[4], M. TEMIZ[5], S. KARAZINCIR[6]

[1]Department of Radiology, Osmaniye State Hospital, Osmaniye, Turkey
[2]Department of Medical Oncology, [3]Department of Pathology, School of Medicine, Hatay Mustafa Kemal University, Hatay, Turkey
[4]Department of Radiology, Hakkari State Hospital, Hakkari, Turkey
[5]Department of General Surgery, [6]Department of Radiology, School of Medicine, Hatay Mustafa Kemal University, Hatay, Turkey

Abstract. – OBJECTIVE: In this study, we aim at investigating the magnetic resonance (MR) imaging features of molecular subtypes, according to the BIRADS Atlas.

PATIENTS AND METHODS: The preoperative MRI examinations of 104 breast cancer patients were reviewed retrospectively using the 5th Edition Breast Imaging-Reporting and Data System (BI-RADS) Atlas. According to BI-RADS, cases were classified as mass or non-mass enhancement. Background parenchymal enhancements of the cases were evaluated. The population was examined for shape, contour, enhancement characteristics of masses, distribution and internal enhancement patterns of non-mass enhancements, background parenchymal enhancement, multifocal/multicentric (MFMS) status, presence of axillary LAP, ADC values, and kinetic aspects. The Kruskal-Wallis and Chi-square tests were used to explore the connection between molecular subtypes and MR data.

RESULTS: The link between molecular subtypes and mass/non-mass enhancement was discovered to be statistically significant (p=0.007). The shape (p=0.001) and contour (p=0.001) properties of the masses were observed to differ depending on the molecular subtypes. The Luminal types were usually irregularly shaped with irregular/spiculated contours, whereas the HER-2 (+) and Triple (-) subtypes were mostly oval/round with smooth contours. The subtype with the highest non-mass enhancement rate (70%) was HER-2 (+). Axillary lymphadenopathy was most common (64.3%) in the Triple (-) subtype (p=0.033).

CONCLUSIONS: According to the BIRADS Atlas, molecular subtypes exhibit a wide range of imaging properties in MR in our study.

Key Words:
BI-RADS, Breast cancer, Magnetic resonance, Molecular subtype, MRI.

Introduction

Breast cancer differs in its presentation, histological features, and clinical course, and molecular subtypes[1-3].

Breast cancer is divided into four major molecular subtypes according to gene expression analysis: Luminal-A, Luminal-B, HER-2 (+), and basal/Triple (-). The inclusion of hormone therapy and targeted medicines based on the identification of molecular subtypes in the treatment strategy have improved survival rates. The disease pattern, response to treatment, prognosis, and survival of molecular subtypes varies. Luminal-A cancers have the best prognosis. They are well-differentiated, have the lowest local recurrence and recurrence rates. Their metastases are most commonly seen in the bones. Luminal-B cancers exhibit worse differentiation, a worse prognosis, and lower levels of ER and PR expression than Luminal-A cancers. Like Luminal-A cancers, Luminal-B cancers metastasize to the bone. Chemotherapeutics (CT) is added to the risk group in Luminal-B along with hormone therapy in the treatment protocol of these two subtypes. HER-2 (+) cancers have a moderate to high nuclear grade. Their metastasis most commonly occurs in the liver and brain. 30 to 40% may also be hormone receptor-positive. The treatment protocol includes HER2-targeting agents and KT. The triple (-) subtype has the worst prognosis of the subtypes. Early relapse risk is high, distant organ metastases are common. Lung and brain are the most common metastases. CT are used in treatment protocols[4-8].

Despite the clinical significance of molecular subtypes, there is no available low-cost genetic

Corresponding Author: Ayça Seyfettin, MD; e-mail: ayca.seyfettin@saglik.gov.tr; aycaseyfettin@hotmail.com

testing yet. Immunohistochemical (IHC) analysis is used to perform molecular subtyping based on ER, PR, HER-2 status, and ki-67 proliferation indicators. While IHC analysis does provide clinical assistance, genetic testing has a 40-100% agreement and has been demonstrated to be less powerful in predicting patient outcomes[9].

As a result, there has been a considerable demand for more accurate techniques to differentiate between molecular subtypes, opening the door for radiogenomics. There is qualitative and quantitative research on MR monitoring features related to molecular subtypes of breast cancer in the literature[10-14].

Breast MRI is the most sensitive imaging method in the diagnosis and preoperative staging of breast cancer[15]. Recent advancements in breast MRI techniques are increasing MRI's relevance in identifying tumor morphology and function[16,17].

The goal of the present study was to investigate the MR imaging properties of molecular subtypes, according to the BIRADS atlas, and thus to answer the question of whether breast MRI can contribute to the treatment plan by assisting with molecular subtype characterization.

Patients and Methods

Patient Population

Between April 2014 and December 2019, 125 cases diagnosed with breast cancer and examined through preoperative breast MRI were studied retrospectively. The study was approved by the Hatay Mustafa Kemal University Clinical Research Ethics Committee with the decision No. 04, dated 05/09/2019.

After excluding 4 patients with recurrent breast cancer, 2 with previous breast operation for other reasons, 2 patients with non-diagnostic MRI examinations, and 13 patients whose pathology results were insufficient for molecular classification, the remaining 104 patients were included in the study.

Imaging and Pathology Data

Informed consent was obtained from the patients before the MRI scans. A 1.5-T MR (Philips Achieva) equipment and a dedicated 7-channel breast coil were used for the MRI, which was performed in the prone position. T1W, T2A, fat-suppressed T2W, dynamic and subtracted (subtractive) dynamic series, DWI were obtained. For T1 A sequences, TR/TE=350-550/8 ms, slice thickness was 3 mm. For T2 A, TR/TE=2500-5000/120 ms, section thickness=3 mm. The 3D FFE THRIVE sequence was used to generate dynamic images, with 6 repetitions at 60-second intervals yielding a total of 7 images, one of which was without contrast. After the gadolinium-containing contrast agent was administered as IV at a dose of 0.1 mmol/kg with an automatic injector, 20 ml of saline infusion was made. Images that change dynamically pre-contrast images on a pixel basis were subtracted from post-contrast images using the subtraction tool which is a standard part of the Philips MR console, and subtracted series were obtained, which aids in ascertaining the contrasting profile. DWI, on the other hand, was obtained by applying the fat suppression technique with TR/TE=1000/84 ms, section thickness=3 mm. Two different b values, b=0 and b=750 mm2/sec, were used for each section.

ADC map images are produced by automatically measuring ADC values on the MR device's console.

Molecular subtyping was done based on the St. Gallen classification[18].

Accordingly, patients were divided into 4 main subtypes according to their ER, PR, HER-2 status, and ki-67 proliferation index (Table I). Subtypes' histological characteristics were recorded.

Evaluation of Images

The MR images of the patients were reviewed at the workstation by two radiologists, one of whom was experienced, without knowing to which molecular subtype they belonged.

The cases were classified as masses or non-mass enhancements according to the 5th Edition BI-RADS Atlas. Morphological (smooth, irregu-

Table I. Breast Cancer Molecular Subtypes.

Molecular Subtype	ER and PR	HER-2	Ki-67
Luminal-A	ER + and/or PR+	HER-2 -	<%14
Luminal-B	ER + and/or PR+/-	HER-2 -	≥%14
	ER + and/or PR+/-	HER-2 +	Any
Her-2 (+)	ER -, PR -	HER-2 +	Any
Triple (-)	ER -, PR -	HER-2 -	Any

Table II. Distribution of BI-RADS traits by molecular subtype.

Molecular Subtype					
	Luminal-A N (%)	Luminal-B N (%)	HER-2 (+) N (%)	Triple (-) N (%)	*p*
Total	27	53	10	14	
Mass or Non-Mass Enhancement					
Mass	17 (63)	43 (80.1)	3 (30)	11 (78.6)	0.007*
NME	10 (37)	10 (19.9)	7 (70)	3 (21.4)	
Background Parenchyma Enhancement					
Minimal	2 (7.4)	5 (9.4)	1 (10)	2 (14.3)	
Mild	7 (25.9)	18 (34.0)	2 (20)	4 (28.6)	0.481
Medium	12 (44.4)	19 (35.8)	4 (40)	4 (28.6)	
Marked	6 (22.2)	11 (20.8)	3 (30)	4 (28.6)	
Mass Shape					
Round	1 (5.9)	3 (7)	1 (33.3)	3 (27.2)	<0.001*
Oval	1 (5.9)	2 (4.7)	2 (66.7)	4 (36.4)	
Irregular	15 (88.2)	38 (88.3)	0 (0)	4 (36.4)	
Mass Contour					
Smooth	2 (11.8)	5 (11.6)	3 (100)	6 (54.5)	0.001*
Irregular	7 (41.2)	22 (51.2)	0 (0)	5 (45.5)	
Spicule	8 (47)	16 (37.2)	0 (0)	0 (0)	
Mass Enhancement Characteristic					
Homogeneous	1 (6.3)	3 (7.1)	0 (0)	1 (9.1)	0.387
Heterogeneous	15 (87.4)	35 (81)	3 (100)	6 (54.5)	
Circular	1 (6.3)	5 (11.9)	0 (0)	4 (36.4)	
Multifocal/Multicentric Involvement					
Yes	7 (25.9)	28 (52.8)	4 (40)	4 (28.6)	0.009
No	20 (74.1)	25 (47.2)	6 (60)	10 (71.4)	

*p-value less than 0.05

lar, spiculated) and enhancement features of the masses (homogeneous, heterogeneous, circular, and non-contracting septa), distribution of non-mass enhancements (focal, linear, segmental, regional, multiple regional, diffuse), and internal contrasting patterns (homogeneous, heterogeneous, consecutive nodular, agglomerated annularly) were evaluated.

Background enhancement, multifocality/multicentricity status, axillary LAP, DAG and kinetic features were evaluated in all cases.

The visual qualitative evaluation of the initial contrast sections classified background parenchymal enhancement as minimum, mild, moderate, or significant[19].

Multiple lesions in the same quadrant were classified multifocal, while multiple lesions in different quadrants or a single lesion greater tha 5 cm were considered multicentric[20]. Pathology results following biopsy or surgery indicated focal, multifocal, multicentric, and contralateral breast involvement.

Axillary lymphadenopathy was characterized as lymph nodes with suspicious morphological features in MRI, such as cortical thickening, rounded form, and increased size, and whose pathologic quality was confirmed by Tru-cut biopsy and/or surgical operation.

The average of the ADC measurements performed using 3 ROIs (regions of interest) from each lesion in mm2/sec was taken while studying the diffusion properties of the lesions. Cystic and necrotic components were avoided when choosing ROI.

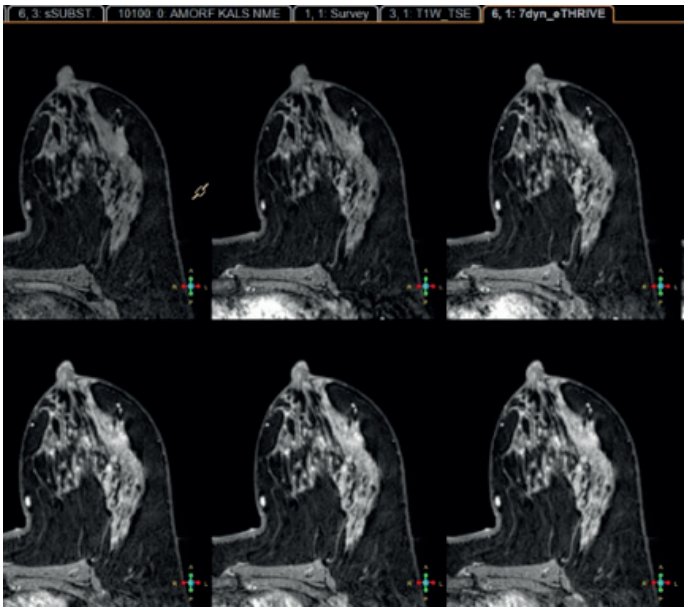

Figure 1. A 49-year-old female patient with HER-2 (+) invasive ductal carcinoma, non-mass enhancement, and segmental distribution on dynamic series.

The kinetic curve was elicited by graphing the intensity-time curves of the lesion signals at the workstation. In the early phase, if the lesion signal intensity grew at a rate of less than 50% in the first 2 minutes, it was noted as slow, between 50-100% was considered medium, and above 100% was considered rapid enhancement. More than 10% increase in persistent augmentation (Type-1 kinetic curve), more than 10% drop wash-out (Type-3 kinetic curve), and more than 10% rise or reduction in signal intensity absence was acknowledged as a plateau in the late phase after the first two minutes (Type-2 kinetic curve)[21].

Statistical Analysis

The research data gained at the conclusion of the study were entered into the Statistical Package for the Social Sciences (SPSS) version 21.0 statistical package program (IBM Corp., Armonk, NY, USA). Controls and analyses of the data were conducted as part of the same program. Frequency (%), mean-median value, standard deviation, maximum and minimum values were used for descriptive statistics in statistical analysis. Kolmogorov-Smirnov and Shapiro-Wilk tests were run in order to confirm data's conformity to the normal distribution. Since data were not compatible with the normal distribution, non-parametric tests were used in the analysis. The Kruskal-Wallis' test and the Chi-square test were employed in comparing the data. In statistical analysis, *p*-values lower than 0.05 were considered significant.

Results

The mean age of 104 patients included in our study was 49.07±9.51 (min=26, max=71). According to their molecular subtypes, 26.0% of the patients were Luminal-A, 50.9% were Luminal-B, 9.6% were HER-2 (+), 13.5% were Triple (-).

Histopathologically, 89 (85.6%) of the patients had invasive ductal carcinoma, 12 (11.5%) had invasive lobular carcinoma, and 3 (2.9%) had medullary carcinoma. 18 Luminal-A, 50 Luminal-B, 12 triple (-), 9 HER-2 (+), invasive lobular carcinomas 9 Luminal-A, 3 Luminal-B, 2 of the medullary carcinomas were triple (-), 1 was HER-2 (+).

There were 74 (71.2%) masses and 30 (28.8%) non-mass enhancing lesions among the lesions. There was a significant correlation between molecular subtypes and mass *vs.* non-mass enhancement, with HER-2 (+) having the highest non-mass enhancement rate (70%, $p=0.007$) (Figure 1).

There was a statistically significant connection between mass shape and contour features and molecular subtypes ($p<0.001$, $p=0.001$). Luminal types were usually irregular in shape and had irregular/spiculated contours (Figure 2), whereas Triple (-) and HER-2 (+) molecular subtypes were mostly oval/round in shape and had smooth contours (Figure 3). There was no significant link ($p=0.387$) between the opposing characteristics and molecular subtypes.

The most prevalent distribution and internal enhancement patterns of non-mass enhancements

were segmental distribution (31%), and heterogeneous enhancement patterns (60%). However, due to the small number of patients, the connection between genetic subtypes and distribution-internal enhancement patterns could not be statistically examined.

Although no statistically significant correlation was found between molecular subtypes and background parenchymal enhancements (p=0.074), Triple (-) and HER-2 (+) tumors had a higher rate (28.6% and 30%, respectively) and significant background parenchymal enhancement compared to Luminal types.

In 42.3%, there was multifocal and/or multicentric involvement. Luminal-B and HER-2 (+) were the most common MFMS subtypes, despite the fact that the relationship between MFMS and subtypes was not statistically significant (p=0.09). Therefore, it could not be statistically analyzed.

The relationship between axillary LAP and molecular subtypes was discovered to be statistically significant (p=0.033). Axillary LAP accompaniment was found to be highest in the Triple (-) (64.3%) subtype.

There was no correlation between ADC values, early-late phase kinetic parameters, and molecular subtypes (p=0.105; 0.105; 0.075, respectively).

Discussion

On MRI, breast cancer might be encountered as a mass or as a non-mass enhancement. Breast cancer was generally observed in the form of mass enhancement in our investigation, which delved into the MR imaging features of molecular subtypes of breast cancer. In parallel with this finding, in a study conducted by Grimm et al[22], 80.9 % of breast tumors were similarly noted as mass enhancement and 19.12% non-mass enhancement. Another study by Vilar et al[23] revealed that 67.8 % were mass augmentation and 32.2% non-mass enhancement. In accordance with these results, in our study, 74 (71.2%) of the cases were observed as masses and 30 (28%) as a non-mass enhancement. Many studies have identified HER-2(+) as the molecular subtype most commonly associated with non-mass enhancement[3,23-35]. This is due to the fact that HER-2 (+) tumors have a higher intraductal component than other subtypes[3]. Likewise, a favorable correlation was discovered in our research between the HER-2 (+) subtype and non-mass augmentation.

Many studies have found that Luminal types typically have irregular shapes and irregular/spiculated contours, whereas Triple (-) and HER-2 (+) subtypes have oval/round shapes and they have been described as having smooth outlines[23,24,26-29]. Similarly, in our study, HER-2 and Triple (-) tumors were mostly smooth, while Luminal types had irregular shape and contour.

The irregular shape and irregular/spiculated contour being more common in Luminal types with a better prognosis are accounted for with the desmoplastic reaction caused by less aggressive, slower growing, lower-stage tumors in the surrounding tissue in order to limit the tumor's growth[30]. The smooth shape and contour property observed in other subtypes are elucidated by the fact that these tumors do not have the time for

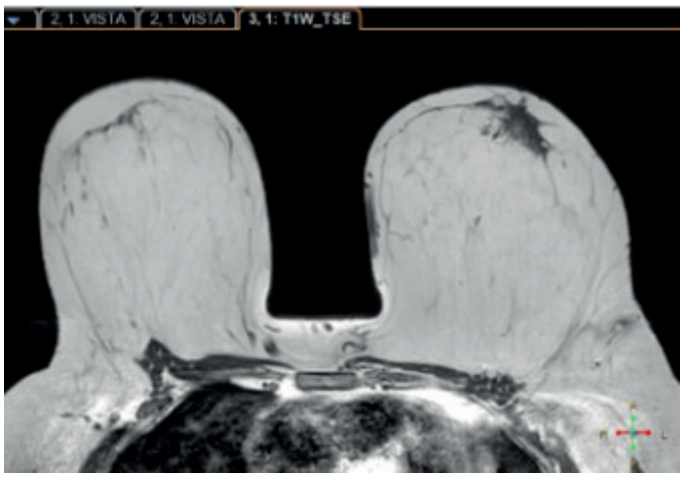

Figure 2. Mass lesion with an irregular shape, spiculated contour on T1W images in a 58-year-old female patient with Luminal–A subtype invasive lobular carcinoma.

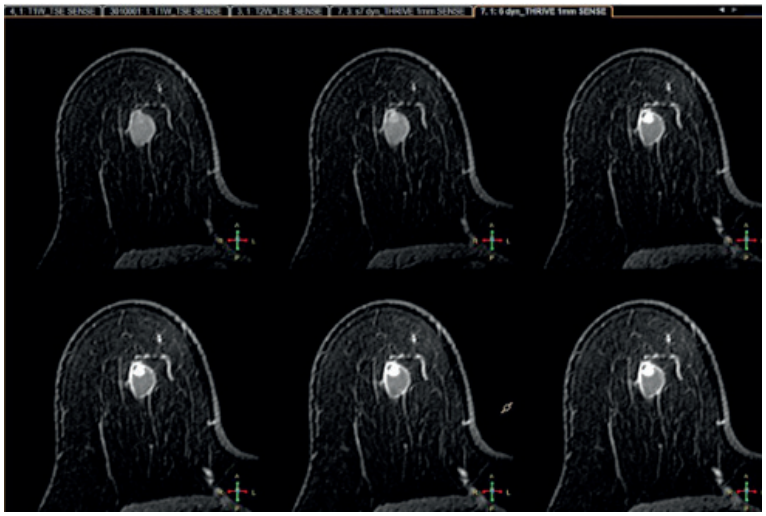

Figure 3. 42-year-old female patient with Triple (-) medullary carcinoma. On dynamic series a round-shaped and well-contoured mass lesion with annular enhancement.

infiltration because of their rapid growth pattern, and that the borders are expanded not by infiltrative but by pushing movement[31].

Many studies[32-35] on non-mass enhancements have shown that the most worrisome distribution pattern for malignancy is segmental, which has been explained by micro invasion of carcinoma and intraductal dissemination. The most common non-mass enhancement distribution pattern in our analysis was segmental. When the internal enhancement patterns of non-mass enhancements have been investigated, numerous studies[33,34,36-38] have concluded that clustered annular and sequential nodular enhancements are the most worrisome in terms of malignancy. The invaded duct and preserved periductal space are shown in clustered annular enhancement, whereas sequential nodular enhancement indicates several ductal structures squashed by fibrous stroma[34]. The most common internal enhancement pattern observed in our study was heterogeneous.

High background parenchymal contrast in breast MRI is thought to be a risk factor for the development of breast cancer, as well as a poor prognosis predictor. It has been reported that enhanced angiogenesis is associated with higher background parenchymal enhancement and microvascular density, both of which have a role in the pathophysiology of carcinogenesis[39,40]. In instances with substantial baseline parenchymal enhancement, unfavorable prognostic characteristics such as delayed diagnosis, aggressive progression, high recurrence rate, and poor response to neoadjuvant treatment have been documented[40-44].

Many studies have shown a correlation between hormone receptor-negative subtypes malignancies with poor prognosis and substantial background parenchymal enhancement[40,44,45]. Although there was no statistically significant correlation between molecular subtypes and background parenchymal enhancement, hormone receptor-negative tumors showed higher background parenchymal enhancement than luminal types in our investigation.

There are numerous studies[28,46-48] in the literature that show a correlation between multifocality/multicentricity and the Luminal-B and HER-2 (+) subtypes.

Although not statistically significant, the subtypes with the highest rates of multifocality/multicentricity in our analysis were Luminal-B and HER-2 (+).

In studies[23,28,46,49,50] investigating the relationship between molecular subtypes and axillary lymphadenopathy, the highest rates of axillary lymphadenopathy positivity were observed in Luminal-B and HER-2 (+) types; however, in a study comparing Luminal-A and B tumors, it was observed in the Luminal-B subtype compared to A[51]. In our study, the most common subtype accompanied by an axillary lymph node was Triple (-) followed by Luminal-B.

It was observed[52-58] that hormone receptor-negative tumors tended to have higher ADC values than positive ones due to increased perfusion secondary to increased angiogenesis, there are significant overlaps between subtypes with studies reporting that HER-2 cancers had the high-

est ADC, HER-2-free Luminal-B group had the lowest ADC values. There was no significant relationship between ADC values and molecular subtypes in our study.

In kinetic analysis, it has been reported that molecular subtypes generally exhibit a heterogeneous kinetic pattern, with studies in the literature indicating that Luminal A and triple-negative tumors exhibit less washout, whereas HER 2 positive tumors exhibit rapid or late washout in the early phase[13,14]. A heterogeneous kinetic model was also observed in our study.

Our study has certain limitations. The retrospective nature of the study, the low proportion of patients falling into subtypes due to the small number of patients, and the absence of use of alternative imaging modalities are all reasons for this.

Conclusions

The studies on breast cancer molecular subtypes are opening a new perspective on breast cancer treatment. So, magnetic resonance could have an increasing role to obtain a fast diagnosis. We need further clinical trials on this issue.

Conflicts of Interest

The authors declare no conflicts of interest.

Funding

Our study does not create additional costs to our hospital. Necessary funding was provided by the authors.

ORCID ID

Ayça Seyfettin: 0000-0002-8540-9432.
İsa Dede: 0000-0002-1836-9370.
Sibel Hakverdi: 0000-0002-1845-6239.
Burcu Düzel Asıg: 0000-0002-6626-1436.
Muhyittin Temiz: 0000-0003-0780-5330.
Sinem Karazincir: 0000-0003-3269-0483.

Conflicts of Interest

The authors declare no conflicts of interest.

References

1) Prat A, Pineda E, Adamo B, Galván P, Fernández A, Gaba L, Díez M, Viladot M, Arance A, Muñoz M. Clinical implications of the intrinsic molecular subtypes of breast cancer. Breast 2015; 24: S26-35.
2) Yerushalmi R, Hayes MM, Gelmon KA. Breast carcinoma—rare types: review of the literature. Ann Oncol 2009; 20: 1763-1770.
3) Boisserie-Lacroix M, Hurtevent-Labrot G, Ferron S, Lippa N, Bonnefoi H, Mac Grogan G. Correlation between imaging and molecular classification of breast cancers. Diagn Interv Imaging 2013; 94: 1069-1080.
4) Kondov B, Milenkovikj Z, Kondov G, Petrushevska G, Basheska N, Bogdanovska-Todorovska M, Tolevska N, Ivkovski L. Presentation of the Molecular Subtypes of Breast Cancer Detected By Immunohistochemistry in Surgically Treated Patients. Open Access Maced J Med Sci 2018; 6: 961-967.
5) Vasconcelos I, Hussainzada A, Berger S, Fietze E, Linke J, Siedentopf F, Schoenegg W. The St. Gallen surrogate classification for breast cancer subtypes successfully predicts tumor presenting features, nodal involvement, recurrence patterns and disease free survival. Breast 2016; 29: 181-185.
6) Brenton JD, Carey LA, Ahmed AA, Caldas C. Molecular classification and molecular forecasting of breast cancer: ready for clinical application? J Clin Oncol 2005; 23: 7350-7360.
7) Foulkes WD, Smith IE, Reis-Filho JS. Triple-Negative Breast Cancer. N Engl J Med 2010; 363:1938-1948.
8) Kaplan HG, Malmgren JA. Impact of Triple Negative Phenotype on Breast Cancer Prognosis. Breast J 2008; 14:456-463.
9) Guiu S, Michiels S, André F, Cortes J, Denkert C, Di Leo A, Hennessy BT, Sorlie T, Sotiriou C, Turner N, Van de Vijver M, Viale G, Loi S, Reis-Filho JS. Molecular subclasses of breast cancer: how do we define them? The IMPAKT 2012 Working Group Statement. Ann Oncol 2012; 23: 2997-3006.
10) Li H, Zhu Y, Burnside ES, Huang E, Drukker K, Hoadley KA, Fan C, Conzen SD, Zuley M, Net JM, Sutton E, Whitman GJ, Morris E, Perou CM, Ji Y, Giger ML. Quantitative MRI radiomics in the prediction of molecular classifications of breast cancer subtypes in the TCGA/TCIA data set. NPJ Breast Cancer 2016; 2: 16012.
11) Grimm LJ, Zhang J, Mazurowski MA. Computational approach to radiogenomics of breast cancer: Luminal A and luminal B molecular subtypes are associated with imaging features on routine breast MRI extracted using computer vision algorithms. J Magn Reson Imaging 2015; 42: 902-907.
12) Mazurowski MA, Zhang J, Grimm LJ, Yoon SC, Silber JI. Radiogenomic analysis of breast cancer: luminal B molecular subtype is associated with enhancement dynamics at MR imaging. Radiology 2014; 273: 365-372.
13) Yamaguchi K, Abe H, Newstead GM, Egashira R, Nakazono T, Imaizumi T, Irie H. Intratumoral heterogeneity of the distribution of kinetic parameters in breast cancer: comparison based on the molecular subtypes of invasive breast cancer. Breast Cancer 2015; 22: 496-502.

14) Blaschke E, Abe H. MRI phenotype of breast cancer: Kinetic assessment for molecular subtypes. J Magn Reson Imaging 2015; 42: 920-924.

15) Vinnicombe S. How I report breast magnetic resonance imaging studies for breast cancer staging and screening. Cancer Imaging 2016; 16: 17.

16) Adrada BE, Candelaria R, Rauch GM. MRI for the Staging and Evaluation of Response to Therapy in Breast Cancer. Top Magn Reson Imaging 2017; 26: 211-218.

17) Miller BT, Abbott AM, Tuttle TM. The influence of preoperative MRI on breast cancer treatment. Ann Surg Oncol 2012; 19: 536-540.

18) Goldhirsch A, Winer EP, Coates AS, Gelber RD, Piccart-Gebhart M, Thürlimann B, Senn HJ; Panel members. Personalizing the treatment of women with early breast cancer: highlights of the St Gallen International Expert Consensus on the Primary Therapy of Early Breast Cancer 2013. Ann Oncol 2013; 24: 2206-2223.

19) Rao AA, Feneis J, Lalonde C, Ojeda-Fournier H. A Pictorial Review of Changes in the BI-RADS Fifth Edition. Radiographics 2016; 36: 623-639.

20) Milulescu A, Di Marino L, Peradze N, Toesca A; -. Management of Multifocal-Multicentric Breast Cancer: Current Perspective. Chirurgia (Bucur) 2017; 112: 12-17.

21) Edwards SD, Lipson JA, Ikeda DM, Lee JM. Updates and revisions to the BI-RADS magnetic resonance imaging lexicon. Magn Reson Imaging Clin N Am 2013; 21: 483-493.

22) 22 Grimm LJ, Zhang J, Baker JA, Soo MS, Johnson KS, Mazurowski MA. Relationships Between MRI Breast Imaging-Reporting and Data System (BI-RADS) Lexicon Descriptors and Breast Cancer Molecular Subtypes: Internal Enhancement is Associated with Luminal B Subtype. Breast J 2017; 23: 579-582.

23) Navarro Vilar L, Alandete German SP, Medina Garcia R, Blanc Garcia E, Camarasa Lillo N, Vilar Samper J. MR Imaging Findings in Molecular Subtypes of Breast Cancer According to BIRADS System. Breast J 2017; 23: 421-428.

24) Song SE, Bae MS, Chang JM, Cho N, Ryu HS, Moon WK. MR and mammographic imaging features of HER2-positive breast cancers according to hormone receptor status: a retrospective comparative study. Acta Radiol 2017; 58: 792-799.

25) Park MJ, Park MY, Kwon JO, Park KS, Yu YB, Yang JH, et al. Clinical Significance of Non-Mass-Like Enhancement of Preoperative Magnetic Resonance Imaging in Breast Cancer Considering Breast-Conserving Surgery. Breast Dis J 2018; 6: 20-24.

26) Çelebi F, Pilancı KN, Ordu Ç, Ağacayak F, Alço G, İlgün S, Sarsenov D, Erdoğan Z, Özmen V. The role of ultrasonographic findings to predict molecular subtype, histologic grade, and hormone receptor status of breast cancer. Diagn Interv Radiol 2015; 21: 448-453.

27) Cho N. Molecular subtypes and imaging phenotypes of breast cancer. Ultrasonography 2016; 35: 281-288.

28) Grimm LJ, Johnson KS, Marcom PK, Baker JA, Soo MS. Can breast cancer molecular subtype help to select patients for preoperative MR imaging? Radiology 2015; 274: 352-358.

29) Uematsu T, Kasami M, Yuen S. Triple-negative breast cancer: correlation between MR imaging and pathologic findings. Radiology 2009; 250: 638-647.

30) Schrading S, Kuhl CK. Mammographic, US, and MR imaging phenotypes of familial breast cancer. Radiology 2008; 246: 58-70.

31) Wojcinski S, Soliman AA, Schmidt J, Makowski L, Degenhardt F, Hillemanns P. Sonographic Features of Triple-Negative and Non–Triple-Negative Breast Cancer. J Ultrasound Med 2012; 31: 1531-1541.

32) Asada T, Yamada T, Kanemaki Y, Fujiwara K, Okamoto S, Nakajima Y. Grading system to categorize breast MRI using BI-RADS 5th edition: a statistical study of non-mass enhancement descriptors in terms of probability of malignancy. Jpn J Radiol 2018; 36: 200-208.

33) Liberman L, Morris EA, Lee MJ, Kaplan JB, LaTrenta LR, Menell JH, Abramson AF, Dashnaw SM, Ballon DJ, Dershaw DD. Breast lesions detected on MR imaging: features and positive predictive value. AJR Am J Roentgenol 2002; 179: 171-178.

34) Tozaki M, Fukuda K. High-spatial-resolution MRI of non-masslike breast lesions: interpretation model based on BI-RADS MRI descriptors. AJR Am J Roentgenol 2006; 187: 330-337.

35) Morakkabati-Spitz N, Leutner C, Schild H, Traeber F, Kuhl C. Diagnostic usefulness of segmental and linear enhancement in dynamic breast MRI. Eur Radiol 2005; 15: 2010-2017.

36) Cho YH, Cho KR, Park EK, Seo BK, Woo OH, Cho SB, Bae JW. Significance of Additional Non-Mass Enhancement in Patients with Breast Cancer on Preoperative 3T Dynamic Contrast Enhanced MRI of the Breast. Iran J Radiol 2016; 13: 30909

37) Liberman L, Morris EA, Dershaw DD, Abramson AF, Tan LK. Ductal Enhancement on MR Imaging of the Breast. AJR Am J Roentgenol 2003; 181: 519-525.

38) Sakamoto N, Tozaki M, Higa K, Tsunoda Y, Ogawa T, Abe S, Ozaki S, Sakamoto M, Tsuruhara T, Kawano N, Suzuki T, Yamashiro N, Fukuma E. Categorization of non-mass-like breast lesions detected by MRI. Breast Cancer 2008; 15: 241-246.

39) Goede V, Fleckenstein G, Dietrich M, Osmers RG, Kuhn W, Augustin HG. Prognostic value of angiogenesis in mammary tumors. Anticancer Res 1998; 18: 2199-2202.

40) Kim JY, Kim SH, Kim YJ, Kang BJ, An YY, Lee AW, Song BJ, Park YS, Lee HB. Enhancement parameters on dynamic contrast enhanced breast MRI: do they correlate with prognostic factors and subtypes of breast cancers? Magn Reson Imaging 2015; 33: 72-80.

41) Hansen NL, Kuhl CK, Barabasch A, Strobel K, Schrading S. Does MRI breast "density" (degree of background enhancement) correlate with mammographic breast density? JMRI 2014; 40: 483-489.

42) Hattangadi J, Park C, Rembert J, Klifa C, Hwang J, Gibbs J, Hylton N. Breast Stromal Enhancement on MRI Is Associated with Response to Neoadjuvant Chemotherapy. AJR Am J Roentgenol 2008; 190: 1630-1636.

43) Kim MY, Cho N, Koo HR, Yun BL, Bae MS, Chie EK, Moon WK. Predicting local recurrence following breast-conserving treatment: parenchymal signal enhancement ratio (SER) around the tumor on preoperative MRI. Acta Radiol 2013; 54: 731-738.

44) Li J, Mo Y, He B, Gao Q, Luo C, Peng C, Zhao W, Ma Y, Yang Y. Association between MRI background parenchymal enhancement and lymphovascular invasion and estrogen receptor status in invasive breast cancer. Br J Radiol 2019; 92: 20190417.

45) Dilorenzo G, Telegrafo M, La Forgia D, Stabile Ianora AA, Moschetta M. Breast MRI background parenchymal enhancement as an imaging bridge to molecular cancer sub-type. Eur J Radiol 2019; 113: 148-152.

46) Ha R, Jin B, Mango V. Breast cancer molecular subtype as a predictor of the utility of preoperative MRI. AJR 2015; 204: 1354.

47) Vera-Badillo FE, Napoleone M, Ocana A. Effect of multifocality and multicentricity on outcome in early stage breast cancer: a systematic review and meta-analysis. Breast Cancer Res Treat 2014; 146: 235.

48) Wiechmann L, Sampson M, Stempel M. Presenting features of breast cancer differ by molecular subtype. Ann Surg Oncol 2009; 16: 2705.

49) Öztürk VS, Polat YD, Soyder A, Tanyeri A, Karaman CZ, Taşkın F. The Relationship Between MRI Findings and Molecular Subtypes in Women With Breast Cancer. Curr Probl Diagn Radiol 2020; 49: 417-421.

50) Sutton EJ, Dashevsky BZ, Oh JH, Veeraraghavan H, Apte AP, Thakur SB, Morris EA, Deasy JO. Breast cancer molecular subtype classifier that incorporates MRI features. J Magn Reson Imaging 2016; 44:122-129.

51) Plaza MJ, Handa P, Esserman LE. Preoperative MRI Evaluation of Axillary Lymph Nodes in Invasive Ductal Carcinoma: Comparison of Luminal A Versus Luminal B Subtypes in a Paradigm Using Ki-67 and Receptor Status. AJR Am J Roentgenol 2017; 208: 910-915.

52) Montemezzi S, Camera L, Giri MG, Pozzetto A, Caliò A, Meliadò G, Caumo F, Cavedon C. Is there a correlation between 3T multiparametric MRI and molecular subtypes of breast cancer? Eur J Radiol 2018; 108: 120-127.

53) Kim SH, Cha ES, Kim HS, Kang BJ, Choi JJ, Jung JH, Park YG, Suh YJ. Diffusion-weighted imaging of breast cancer: correlation of the apparent diffusion coefficient value with prognostic factors. J Magn Reson Imaging 2009; 30: 615-620.

54) Nakajo M, Kajiya Y, Kaneko T, Kaneko Y, Takasaki T, Tani A, Ueno M, Koriyama C, Nakajo M. FDG PET/CT and diffusion-weighted imaging for breast cancer: prognostic value of maximum standardized uptake values and apparent diffusion coefficient values of the primary lesion. Eur J Nucl Med Mol Imaging 2010; 37: 2011-2020.

55) Sun K, Chen X, Chai W, Fei X, Fu C, Yan X, Zhan Y, Chen K, Shen K, Yan F. Breast Cancer: Diffusion Kurtosis MR Imaging-Diagnostic Accuracy and Correlation with Clinical-Pathologic Factors. Radiology 2015; 277: 46-55.

56) Jeh SK, Kim SH, Kim HS, Kang BJ, Jeong SH, Yim HW, Song BJ. Correlation of the apparent diffusion coefficient value and dynamic magnetic resonance imaging findings with prognostic factors in invasive ductal carcinoma. J Magn Reson Imaging 2011; 33: 102-109.

57) Sharma U, Sah RG, Agarwal K, Parshad R, Seenu V, Mathur SR, Hari S, Jagannathan NR. Potential of Diffusion-Weighted Imaging in the Characterization of Malignant, Benign, and Healthy Breast Tissues and Molecular Subtypes of Breast Cancer. Front Oncol 2016; 6: 126.

58) Xie T, Zhao Q, Fu C, Bai Q, Zhou X, Li L, Grimm R, Liu L, Gu Y, Peng W. Differentiation of triple-negative breast cancer from other subtypes through whole-tumor histogram analysis on multiparametric MR imaging. Eur Radiol 2019; 29: 2535-2544.